Materials Research Proceedings 41 (2024) 715-722 https://doi.org/10.21741/9781644903131-79

# Characterization and modelling of grain growth in Zr-Nb alloys: Niobium concentration influence

HAHN Pauline[1,2,a *], GAILLAC Alexis[2], FLIPON Baptiste[1], BIGNON Madeleine[1], BOZZOLO Nathalie[1] and BERNACKI Marc[1]

[1]Mines Paris – PSL, CNRS, CEMEF, UMR 7635, France

[2]Framatome – Components Research Center, France

[a]pauline.hahn@minesparis.psl.eu

**Keywords:** Zr-Nb Alloys, Grain Growth, Solute Drag, Numerical Simulation

**Abstract.** Zr-Nb alloys are mainly used in the nuclear energy industry. A study was carried out with the aim of understanding the physical phenomena involved during the hot extrusion stage and modeling these phenomena with numerical simulations. However, it is first essential to determine the material parameters, including reduced mobility during pure grain growth. Experimental and numerical campaigns are therefore carried out to define this parameter, material and model dependent. Consequently, this study focuses exclusively on the influence of niobium content on the grain growth kinetics of Zr-Nb alloy.

## Introduction

In nuclear fuel assemblies, zirconium alloys are mainly used due to their low neutron capture cross section. These alloys fulfill the high requirements of nuclear applications regarding good mechanical properties and corrosion resistance in relation to their in-use environment (mainly cladding tubes and structural components of fuel assemblies located in the nuclear power plant core) [1]. The material properties are determined by their microstructure, which evolves during the manufacturing process. In this work, the interest is focused on the hot extrusion stage to study recrystallization (ReX) and grain growth (GG) kinetics in Zr-Nb alloys. In the literature, alloying elements, including niobium, have been reported to strongly impact ReX and related phenomena [2]. The commercial Zr-1Nb alloy showed some difficulty in recrystallizing after hot extrusion. In order to understand the physical phenomena involved, a first stage consists of studying and quantifying the influence of niobium on GG kinetics on Zr-Nb alloy, composed of an α matrix (hexagonal close-packed) and of a β phase (body-centered cubic) considered as second phase particles population [3]. Experimental heat treatments were done to first obtain a fully recrystallized microstructure and then carry out annealing at different temperatures. Alloying elements such as niobium can segregate at grain boundaries (GB). During GG, if the diffusion coefficient of these segregated elements in the matrix is slower than the GB migration velocity, these elements will have an impact on the GB migration kinetics, known as solute drag effect [4]. Moreover, samples with 1% of niobium are analyzed to identify the Smith Zener pinning pressure associated with second phase particles [4,5,6]. Experimental characterizations were performed to be able to model the GG kinetic with predictive full-field simulations based on a level-set description of the GB [7].

## Materials and methods

The Zr-1Nb alloy contains several alloying elements, of which niobium is the main element at 1% by weight. To determine GG kinetics, a single-phase material (without second phase particles) must be considered. Consequently, small ingots of approximately 1.7 kg were produced with different niobium contents in order to identify the influence of niobium in solid solution on GG kinetics. It was considered 0 - 0.2 - 0.4% of niobium by mass. 0.4% of niobium corresponds to the

solubility limit of niobium in the α phase at 580°C. An ingot with 1% of niobium was also produced to take into account the impact of second phase particles on GG kinetics. Each ingot contains around 1400 ppm of oxygen and 300 ppm of iron. Fig. 1 illustrates the manufacturing process used to obtain sheets of about 3mm thick and from which 5x5mm samples are taken. It should be noted that the reduction ratio of the last cold rolling pass is 50%.

The last heat treatment duration at 580°C in Fig. 1 was adapted for each niobium content in order to begin GG heat treatments from a fully recrystallized state. Static recrystallization kinetics are also influenced by the niobium content. According to microhardness tests on a Zr-1Nb sheet

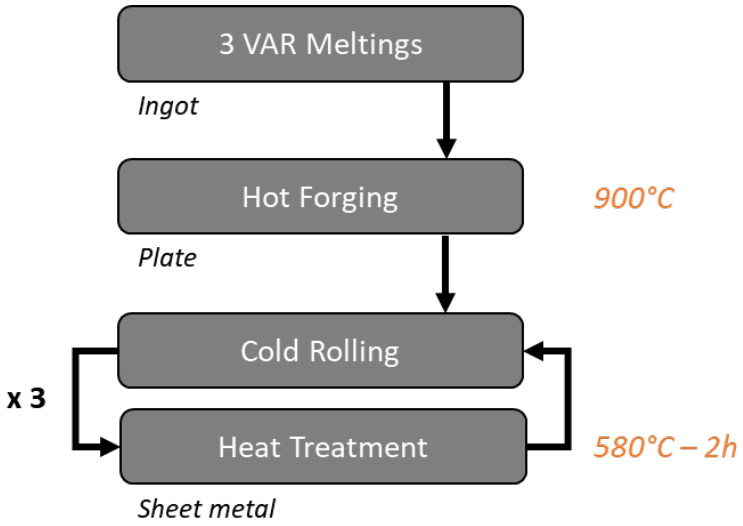


*Fig. 1. Sheet metal manufacturing process for this study.*

presented by Tian et al. [8], 140 minutes are required to obtain a fully recrystallized material after heat treatment at 580°C. The reduction rate of this sheet is 50%, identical to the reduction rate of the samples in this study. An experimental matrix was defined to track the evolution of the recrystallized fraction between the initial state and 150 minutes of heat treatment at 580°C for each niobium content. ReX and GG annealing temperatures were fixed to avoid moving into the two-phase α + β domain. This temperature is around 600°C. 580°C allows an overshoot margin for the furnace during the beginning of the heat treatment. After defining the fully recrystallized metallurgical state as a function of niobium content, GG annealings were carried out. This curvature flow mechanism is thermally activated and driven by the minimization of the total surface energy of the system, leading to a decrease of the GB network length [4]. This experimental and numerical campaign will highlight the influence of niobium on GG kinetics. The material parameters dependent on the numerical model used will also be determined, in particular the GB mobility. Therefore, 3 heat treatment temperatures are considered, and for each temperature at least 3 durations to use Burke and Turnbull's law [9]. The experimental matrix was adapted following the first results. A complete matrix has been defined for the Zr-0Nb samples with at least 3 heat treatment durations at 530°C, 550°C and 580°C. Results from samples with 0.2% and 0.4% of niobium will be used to identify the niobium solute drag effect on grain growth. The solute drag effect involves the impact of some alloying elements in solid solution on the velocity of GB migration [4]. Research by Zahler et al. [10] highlights this phenomenon.

## Experimental procedure

In order to determine the recrystallized fraction in the samples resulting from the ReX heat treatment, EBSD analysis was selected. To obtain statistically significant data, it was decided to use a view field of 500 µm wide and 375 µm high with a measurement step of 500 nm. The recrystallized fraction criterion was then defined with a GAKAM (grain average kernel average misorientation) value of less than 0.4° to consider a recrystallized grain. To characterize grain size after GG annealing, optical microscope images were taken under polarized light. This method was chosen to save time compared with EBSD analysis. During the final metallographic preparation stage, a thin oxide layer is created on the surface. Under polarized light, the surface is reflected in different ways depending on the crystallographic orientation of the grains. A view field of 330 µm wide and 250 µm high is considered. In order to be able to discretise the different crystallographic orientations during image post-processing, 3 images were taken of the same area with a different polarization, as shown in Fig. 2. In addition, in order to be representative of the sample, 3 observation zones are also recommended. The article by Flipon et al. [11] explains the method used via the Fiji software [12]. A step in the Fiji image post-processing macro also recorded information on the area of each grain captured. Grains without a closed outline are not taken into account. The equivalent circle diameter (ECD) can therefore be calculated. The ECD for a grain is calculated using Eq. 1.

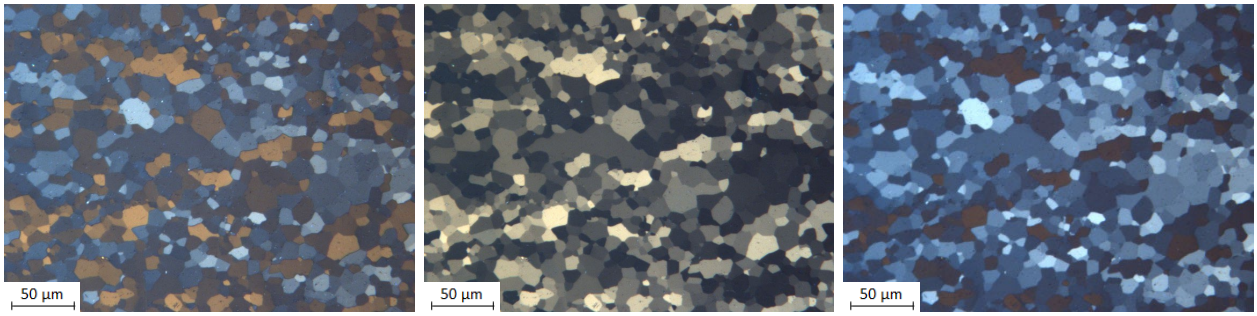


*Fig. 2. Images of the same area with a different polarisation. View field of 330 µm wide.*

$$ECD_i = 2\sqrt{\frac{A_i}{\pi}} \tag{1}$$

with $A_i$ the area of a grain. Subsequently, an average ECD value can be calculated from the individual ECDs as Eq. 2.

$$\overline{ECD} = \frac{1}{N}\sum_{i=1}^{N} ECD_i \tag{2}$$

with $N$ the total number of grains studied. A comparison was carried out between the average grain size obtained using EBSD maps (reference values) and the average grain size obtained using this method of optical observation and post-processing. The results are similar. The number of grains taken into account in this analysis (at least 1500 grains) gives statistical results for the average grain size of the sample.

## Numerical simulations

The microstructural evolution associated with ReX and GG can be modeled in several ways. In our case, full-field simulations based on a level-set (LS) description of the GB were chosen [7]. These simulations are highly accurate, providing an explicit microstructure description of local phenomena. Using the experimental results of this campaign, it is possible to model the GG

kinetics in the DIGIMU software [13]. The microstructure was generated by immersing an experimental image with around 900 grains. The GB migration velocity is expressed in Eq. 3 [4].

$$\vec{v} = MP\vec{n} \tag{3}$$

with $M$ the grain boundary mobility ($M = 1.7 \times 10^{-3}$ mm$^4$/J.s for simulation with 0% of niobium at 580°C), $P$ the sum of the driving pressures applied on the GB and $\vec{n}$ the unit normal exiting at the GB. In the case of GG, the term $P$ in Eq. 4 refers only to the capillary pressure term $P_c$ [4] and can be considered as a first approximation.

$$P = P_c = -\gamma\kappa \tag{4}$$

where $\gamma$ corresponds to the GB energy (in our case, values taken from the literature [14] for Zircaloy-4) and $\kappa$ is the mean GB curvature (trace of the curvature tensor in 3D). Then, GB mobility can be expressed as follows in Eq. 5 using an Arrhenius law.

$$M = M_0 \, exp\left(\frac{-Q}{RT}\right) \tag{5}$$

with $M_0$ the preexponential constant factor, $Q$ the mobility activation energy, $R$ the perfect gas constant and $T$ the absolute temperature. The model selected for the solute drag effect for 0.2% and 0.4% of niobium will be described in more details in the following section.

**Results and discussion**

By post-processing images taken with an optical microscope under polarized light, a grain size distribution was obtained for each sample (heat treatment time and niobium content) and an average grain size in diameter (ECD) was determined. Fig. 3 illustrates the different kinetics obtained as a function of niobium content with a heat treatment temperature of 580°C. GG kinetics decreased with increasing niobium content. A significant difference was observed between 0.2% and 0.4% of niobium. Furthermore, with 0% of niobium, the kinetics of GG are still low compared with other materials, due to the low heat treatment temperature for GG. However, to remain in the single-phase range, the heat treatment temperature cannot be higher. A threshold is quickly reached after 4 to 8 hours of heat treatment, even with 0% of niobium. The presence of other elements, such as oxygen in solid solution, as well as the presence of iron, could be the reason for this plateau. A parallel investigation is underway on pure zirconium samples in order to detect the possible solute drag effect of oxygen. The results for different heat treatment temperatures for 0% of niobium are exhibited in Fig. 4. This graph shows how GG kinetics decrease with decreasing temperature. These data will be used to estimate a reduced mobility value for each temperature using Burke and Turnbull's law [9].

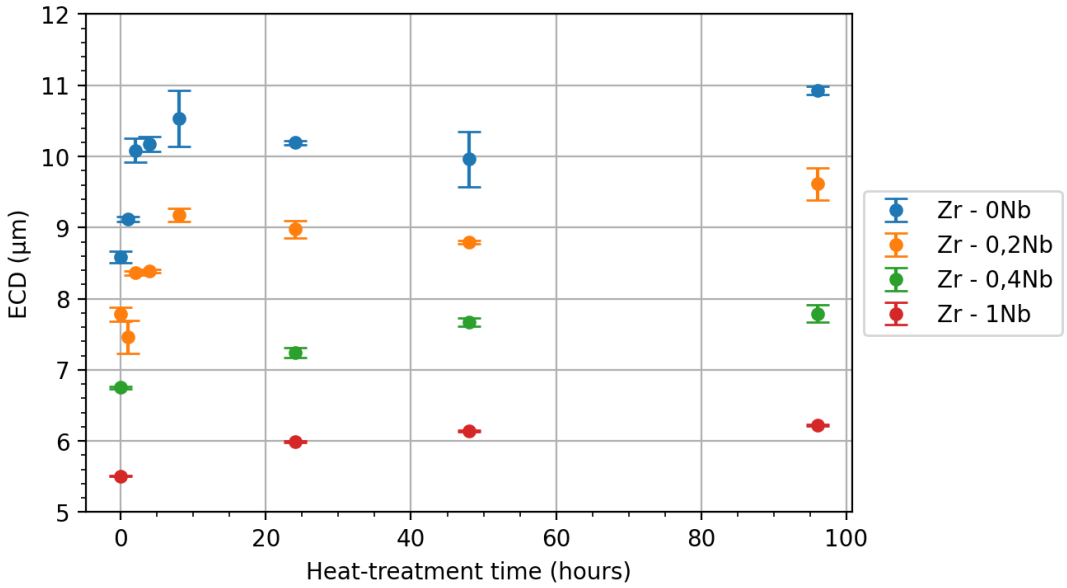


*Fig. 3. ECD evolution as a function of heat treatment time and niobium content at 580°C.*

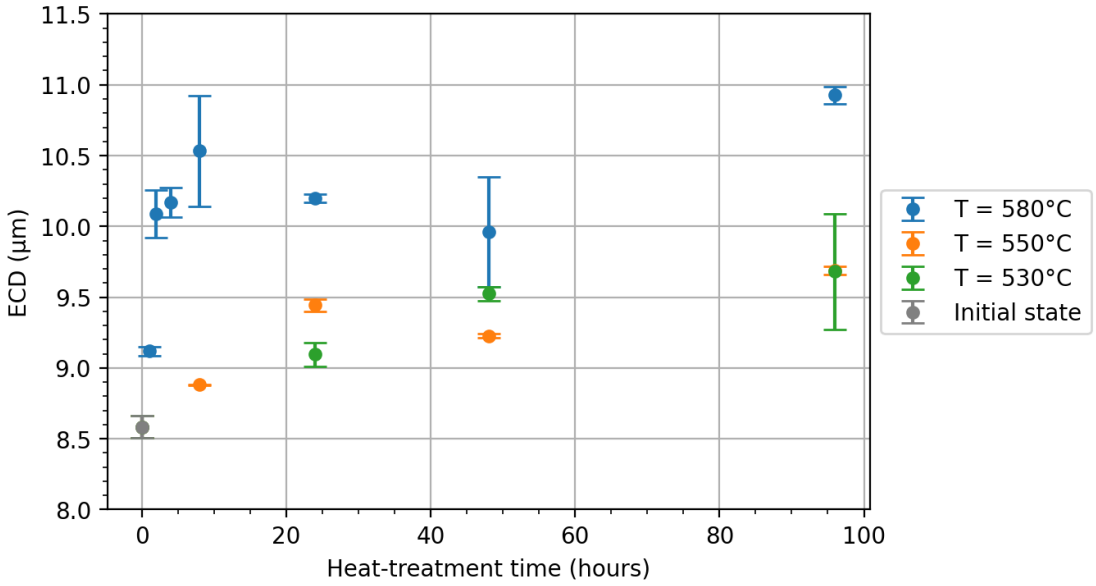


*Fig. 4. ECD evolution as a function of different heat treatment temperature for 0% of niobium.*

Given the threshold observed on the experimental data at 580°C with 0% of niobium (see Fig.4), the reduced mobility was estimated only on the first experimental points, from the initial state to 8 hours of heat treatment. Full-field numerical simulations were carried out with the estimated value of reduced mobility. This value was subsequently readjusted following the initial simulation results because of its dependence on the material and the numerical model used. The simulation results following readjustment of the parameter are shown in Fig. 5. Considering the low mobility value and the grain size heterogeneity, it is necessary to immerse an experimental image to obtain GG kinetics coherent with the experimental results.

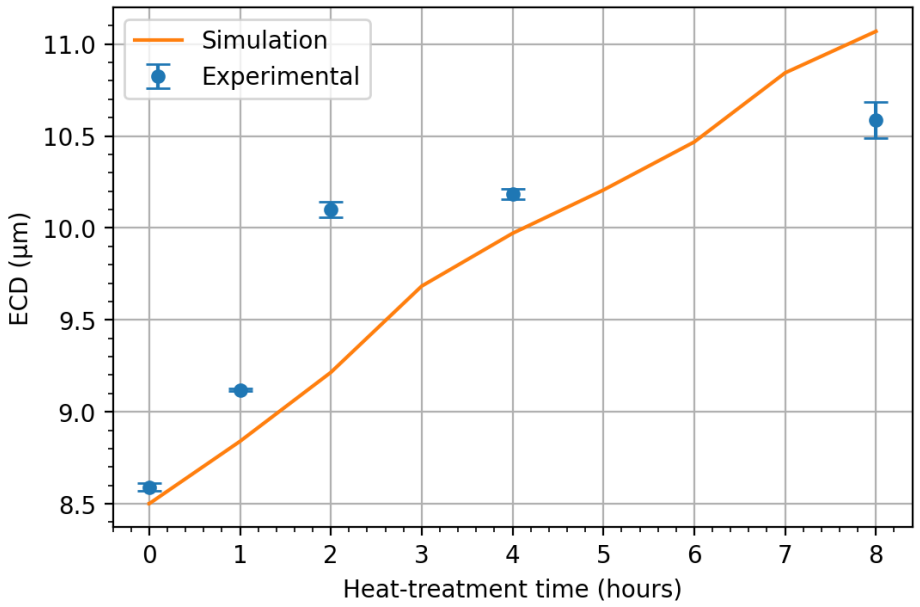


*Fig. 5. Grain growth kinetics comparison between experimental and simulation data for Zr-0Nb at 580°C.*

Consequently, around 900 grains are taken into account, which does not provide a representative picture of the microstructure evolution. In the simulations, the average grain size is calculated in the same way as the experimental data, considering only "closed" grains. With a solute drag effect (results with 0.2 and 0.4% niobium), Burke and Turnbull's law [9] cannot be predictive of GG kinetics. At mesoscopic scale, the solute drag effect is usually incorporated into the mobility parameter by modifying the apparent activation energy or by applying an additional driving pressure known as solute pressure. In the literature, full-field simulations based on a level-set description of GB has not been found to model solute drag effect in metallic materials. The Cahn-Lücke-Stüwe model [15,16,17] was firstly adopted to represent the solute drag effect in Zr-Nb alloys to improve the representativity of full-field simulations [18]. The principle consists in adding, in the convective part of the level-set (LS) transport equations, a velocity-dependent pinning pressure $P_i$ to the GB migration velocity as described in Eq. 6 and Eq. 7.

$$P = P_c + P_i \tag{6}$$

$$P_i = \frac{\alpha\, v\, C_0}{1+\beta^2 v^2} \tag{7}$$

with $v$ the GB velocity, $C_0$ the concentration of alloying element, $\alpha$ and $\beta$ material parameters to be identified. The pinning pressure (cf. Eq. 7) can thus be added to the global equation (cf. Eq. 3) to define the GB migration velocity taking into account the solute drag effect [15]. For this reason, the Cahn-Lücke-Stüwe (CLS) model will be used to add a pinning pressure (homogeneous in all the material) in order to reduce the GB migration velocity. At the same time, a solute drag effect due to oxygen is probably present in samples with 0% of niobium as illustrated in Fig. 5 and will be confirmed by comparing GG results with pure zirconium.

**Summary**

In this work, the characterization and modelling of GG kinetics in Zr-Nb alloys were studied. The influence of niobium content was highlighted based on experimental investigations. The conclusions and prospects of this study are summarised as follows:

- Numerical simulations for grain growth were conducted and reduced mobility was identified for 0% of niobium content.
- The influence of niobium content has been observed on ReX and GG kinetics.
- Oxygen content in solid solution seems to influence GB migration velocity.
- In future work, CLS model will be adapted to take into account the impact of the solute drag effect due to niobium in solid solution.
- Second phase particles will be included in numerical simulations to compare with experimental results with 1% of niobium.

**References**

[1] D. O. Northwood, The development and applications of zirconium alloys, Materials & Design, 6 (1985) 58–70. https://doi-org /10.1016/0261-3069(85)90165-7

[2] H. Yang, J. Shen, and Y. Matsukawa, Effects of alloying elements (Sn, Nb, Cr and Mo) on the microstructure and mechanical properties of zirconium alloys, Journal of Nuclear Science and Technology, 52 (2015) 1162–1173. https://doi.org/10.1080/00223131.2014.996622

[3] A. Gaillac, Mise en forme des alliages de zirconium et de hafnium, Techniques de l'Ingénieur, M3190(V1) (2018). https://doi.org/10.51257/a-v1-m3190

[4] J. Humphreys, G. S. Rohrer, and A. Rollett, Recrystallization and Related Annealing

Phenomena, Materials Science and Engineering, Elsevier, third edition, 2017.

[5] C. S. Smith, Introduction to grains, phases, and interfaces – an interpretation of microstructure, Transaction metallurgy Society of AIME, 175 (1948) 15–51.

[6] C. Zener, Theory of growth of spherical precipitates from solid solution, Journal of Applied Physics, 20 (1949) 950–953.

[7] M. Bernacki, R. E. Logé, and T. Coupez, Level set framework for the finite-element modelling of recrystallization and grain growth in polycrystalline materials, Scripta Materialia, 64 (2011) 525–528. https://doi.org/10.1016/j.scriptamat.2010.11.032

[8] H. Tian, X. Wang, W. Gong, J. Zhou, and H. Zhang, Recrystallization behavior of cold-rolled Zr–1Nb alloy, Journal of Nuclear Materials, 456 (2015) 321–328. https://doi.org/10.1016/j.jnucmat.2014.09.084

[9] J. E. Burke and D. Turnbull, Recrystallization and grain growth, Progress in Metal Physics, 3 (1952) 220–292. https://doi.org/10.1016/0502-8205(52)90009-9

[10] M. P. Zahler, S. M. Kraschewski, H. Störmer, D. Gerthsen, M. Bäurer, and W. Rheinheimer, Grain growth and segregation in Fe-doped SrTiO3: Experimental evidence for solute drag, Journal of the European Ceramic Society, 43 (2023) 1613–1624. https://doi.org/10.1016/j.jeurceramsoc.2022.11.074

[11] B. Flipon, V. Grand, B. Murgas, A. Gaillac, A. Nicolaÿ, N. Bozzolo, and M. Bernacki, Grain size characterization in metallic alloys using different microscopy and post-processing techniques, Materials Characterization, 174 (2021) 1–14. https://doi.org/10.1016/j.matchar.2021.110977

[12] J. Schindelin, I. Arganda-Carreras, E. Frise, V. Kaynig, M. Longair, T. Pietzsch, S. Preibisch, C. Rueden, S. Saalfeld, B. Schmid, J.-Y. Tinevez, D. James White, V. Hartenstein, K. Eliceiri, P. Tomancak, and A. Cardona, Fiji: an open-source platform for biological-image analysis, Nature Methods, 9 (2012) 676–682. https://doi.org/10.1038/nmeth.2019

[13] Transvalor, DIGIMU Software, Read on https://www.transvalor.com/en/digimu the 10 December 2023.

[14] J. W. C. Dunlop, Y. J. M. Bréchet, L. Legras, and H. S. Zurob, Modelling isothermal and non-isothermal recrystallisation kinetics: Application to Zircaloy-4, Journal of Nuclear Materials, 366 (2007) 178–186. https://doi.org/10.1016/j.jnucmat.2006.12.074

[15] J. W. Cahn, The impurity-drag effect in grain boundary motion, Acta Metallurgica, 10 (1962) 789–798. https://doi.org/10.1002/9781118788295.ch16

[16] K. Lücke and H. P. Stüwe, Recovery and Recrystallization of Metals, Interscience by L. Himmel edition, 1963.

[17] K. Lücke and H. P. Stüwe, On the theory of impurity controlled grain boundary motion, Acta Metallurgica, 19 (1971) 1087–1099. https://doi.org/10.1016/0001-6160(71)90041-1

[18] J. Furstoss, C. Petit, A. Tommasi, C. Ganino, D. Muñoz, M. Bernacki, On the role of solute drag in reconciling laboratory and natural constraints on olivine grain growth kinetics, Geophysical Journal International, 224 (2021) 1360–1370. https://doi.org/10.1093/gji/ggaa520